

Article

LAP and IRS Enhanced Secure Transmissions for 6G-Oriented Vehicular IoT Services

Lingtong Min¹, Jiawei Li¹ , Yixin He^{2,*}  and Qin Si³

¹ School of Electronics and Information, Northwestern Polytechnical University, Xi'an 710072, China; minlingtong@nwpu.edu.cn (L.M.); jiawei-li@mail.nwpu.edu.cn (J.L.)

² College of Information Science and Engineering, Jiaxing University, Jiaxing 314001, China

³ Changji Electric Power Supply Company, State Grid Xinjiang Electric Power Co., Ltd., Changji 831100, China; tbea_18599330971@163.com

* Correspondence: yixinhe@zjxu.edu.cn

Abstract: In 6G-oriented vehicular Internet of things (IoT) services, the integration of a low altitude platform (LAP) and intelligent reflecting surfaces (IRS) provides a promising solution to achieve seamless coverage and massive connections at low cost. However, due to the open nature of wireless channels, how to protect the transmission of privacy information in LAP-based IRS symbiotic vehicular networks remains a challenge. Motivated by the above, this paper investigates the LAP and IRS enhanced secure transmission problem in the presence of an eavesdropper. Specifically, we first deploy a fixed LAP equipped with IRS to overcome the blockages and introduce artificial noise against the eavesdropper. Next, we formulate a total secure channel capacity maximization problem by optimizing the phase shift, power distribution coefficient, and channel allocation. To effectively solve the formulated problem, we design an iterative algorithm with polynomial complexity, where the optimization variables are solved in turn. In addition, the complexity and convergence of the proposed iterative algorithm are analyzed theoretically. Finally, numerical results show that our proposed secure transmission scheme outperforms the comparison schemes in terms of the total secure channel capacity.

Keywords: intelligent reflecting surfaces (IRS); low-altitude platform (LAP); secure transmission; total secure channel capacity; vehicular Internet of things (IoT) services



Citation: Min, L.; Li, J.; He, Y.; Si, Q. LAP and IRS Enhanced Secure Transmissions for 6G-Oriented Vehicular IoT Services. *Drones* **2023**, *7*, 414. <https://doi.org/10.3390/drones7070414>

Academic Editor: Carlos Tavares Calafate

Received: 26 May 2023
Revised: 15 June 2023
Accepted: 20 June 2023
Published: 22 June 2023



Copyright: © 2023 by the authors. Licensee MDPI, Basel, Switzerland. This article is an open access article distributed under the terms and conditions of the Creative Commons Attribution (CC BY) license (<https://creativecommons.org/licenses/by/4.0/>).

1. Introduction

While the dense coverage of fifth-generation (5G) terrestrial networks can satisfy the demands of vehicular Internet of things (IoT) services in hotspots, people still have urgent requirements for ubiquitous connectivity with high data rates in remote areas [1]. Due to the inherent limitations of terrestrial networks, air-to-ground (A2G) communications are envisioned as a promising technique to serve sixth-generation (6G)-oriented vehicular IoT applications [2–4]. As the most representative A2G communications, low-altitude platform (LAP)-enhanced transmissions have lower path loss and higher line-of-sight (LoS) link probability, which can be deployed on demand via a levitation mode to provide seamless and flexible coverage [5–7]. On the other hand, intelligent reflecting surfaces (IRS) with low hardware cost and power consumption can be used for 6G-oriented vehicular IoT services by smartly reconfiguring wireless propagation environments [8–10].

Following the technological advancements of A2G communications, the combination of LAP and IRS has attracted a certain amount of attention [11]. Generally, this combination can be divided into two cases, i.e., mobile IRS schemes [12,13] and fixed IRS schemes [14–16]. However, in some practical vehicular network (VNet) scenarios (e.g., emergency rescues), mobile IRS schemes may be impractical. The reason is that the payload and flight time of LAPs with mobile capability are extremely limited. According to the above discussion, the authors in [14] derived the channel gain lower bound for LAP and IRS collaborative

communications. Inspired by this work, the researchers in [15] investigated the sum rate maximization problem of LAP-aided IRS networks by optimizing the phase shift and LAP altitude. Moreover, by using quasi-stationary LAPs, the IRS-assisted multi-layer aerial architecture was proposed in [16], which pointed out a promising direction for 6G-oriented vehicular IoT services. Furthermore, in order to improve the channel capacity, more works focused on the network optimization problems, including beamforming, resource (e.g., power and spectrum) allocation, and energy efficiency optimization [17–20]. We have summarized these works in Table 1.

Table 1. Summary of key contributions and limitations of existing works on UAV-aided RIS-assisted IoT networks.

Reference	Key Contributions	Limitation
[14]	The channel gain lower bound for LAP and IRS collaborative communications was derived.	
[15]	The sum rate maximization problem of LAP-aided IRS networks was investigated, where the phase shift and LAP altitude were optimized.	These works make an implicit assumption that LAP-based IRS symbiotic vehicular networks (VNets) are secure. In LAP-based IRS symbiotic VNets, the privacy information is susceptible to eavesdropping due to the open nature of A2G channels.
[16]	The IRS-assisted multi-layer aerial architecture was proposed.	
[17–20]	By considering the beamforming, resource allocation, and energy efficiency, the channel capacity was improved.	

Although the above works present optimization policies and models of LAP and IRS enhanced transmissions, these works make an implicit assumption that LAP-based IRS symbiotic vehicular networks (VNets) are secure. In LAP-based IRS symbiotic VNets, the privacy information is susceptible to eavesdropping due to the open nature of A2G channels [21]. Traditionally, the network security is protected by upper-layer encryption methods. However, such encryption algorithms and key allocation strategies will significantly improve the complexity of the system [22]. Faced with the above challenges, by using the wireless channel characterizations, the physical layer security (PLS) technique can be regarded as a promising alternative technique, which can be widely applied to 6G-oriented vehicular IoT services to ensure information security [23]. Therefore, under the constraints of network security, how to improve the total secure channel capacity of LAP and IRS enhanced transmissions is a key technical difficulty.

Motivated by the above, this paper investigates the secure transmission problem in LAP-based IRS symbiotic VNets in the presence of an eavesdropper. First, we deploy a fixed LAP equipped with IRS to overcome the blockages and exploit artificial noise (AN) to interfere with the eavesdropper. Next, aiming to maximize the total secure channel capacity, we formulate this problem as a mixed-integer and non-convex program. To effectively solve the formulated problem, an iterative algorithm with polynomial complexity is proposed, where the phase shift, power distribution coefficient, and channel allocation are optimized in turn. Then, we theoretically analyze the complexity and convergence of the proposed iterative algorithm. Finally, numerical results show that the proposed secure transmission scheme significantly improves the total secure channel capacity against the current works [2,23] and baseline scheme. In addition, the influence of the number of reflection elements is discussed. The above results are a meaningful guide for improving the quality of service (QoS) of 6G-oriented vehicular IoT services.

The rest of this article is organized as follows. Section 2 introduces the network model and presents the total secure channel capacity maximization problem. Then, in Section 3, we design an iterative algorithm with polynomial complexity to solve the formulated problem. Simulation results are presented in Section 4. Finally, Section 5 concludes the paper.

2. Network Model and Problem Formulation

Figure 1 illustrates the considered LAP-based IRS symbiotic VNet, which consists of a remote base station (RBS), a fixed LAP equipped with IRS, U legitimate vehicle users, and an eavesdropper. The set of legitimate vehicle users is denoted as $\mathcal{U} = \{1, 2, \dots, U\}$. We assume that there is no direct communication link between the RBS and the legitimate vehicle user/eavesdropper due to obstacles [8]. Under this condition, we adopt the LAP equipped with IRS to enhance transmissions. The IRS can be controlled by an intelligent controller.

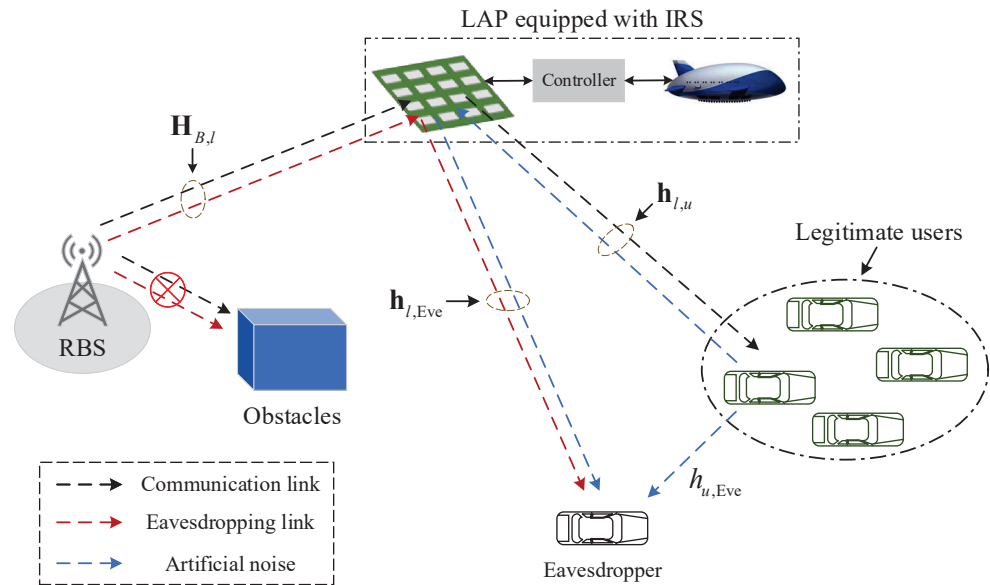


Figure 1. LAP-based IRS symbiotic VNet.

It is assumed that the IRS has G_h horizontal reflection elements and G_v vertical reflection elements, denoted as $\mathcal{G} = \{1, 2, \dots, G\}$, where $G = G_h \times G_v$. Moreover, the RBS has N antennas and K channels, denoted as $\mathcal{K} = \{1, 2, \dots, K\}$, where $K \geq U$. Let $\mathbf{K} = \{k_u | \forall k \in \mathcal{K}, \forall u \in \mathcal{U}\}$ denote the channel allocation policy. If the u -th ($\forall u \in \mathcal{U}$) legitimate vehicle user occupies the k -th ($\forall k \in \mathcal{K}$) channel, $k_u = 1$; otherwise, $k_u = 0$. Furthermore, each legitimate vehicle user with self-interference cancellation capability has two antennas that can implement full-duplex communication. Meanwhile, we assume that the AN emitted by the legitimate vehicle users will not affect the received signals, and the eavesdropper is equipped with a single antenna [24]. Since the total power P_u^{\max} of the system is limited, the RBS and the u -th legitimate vehicle user need to negotiate to decide the transmitted power P_u^{down} of RBS (downlink) and the transmitted power P_u^{up} of AN (uplink). Especially, as discussed in [21], the channel is assumed to have reciprocity. Likewise, it is assumed that the channel state information (CSI) associated with the eavesdropper/IRS is available. The reason is that even for a passive eavesdropper, it can also estimate its CSI through local oscillator power inadvertently leaked from the eavesdropper’s receiver radio frequency frontend [25]. Since the investigated scenario is highly dynamic, imperfect estimation of the reflection phases and phase errors are possible with respect to the link between LAP and ground nodes. In this situation, the CSI of the LAP vehicle links needs to be periodically reported to the RBS with a feedback period. According to [26], the first-order Gauss–Markov process can be utilized to estimate the CSI of LAP-vehicle links.

According to the above description, the received signal y_u of the u -th legitimate vehicle user can be expressed as

$$y_u = \mathbf{h}_{I,u}^H \Phi \mathbf{H}_{B,I} P_u^{\text{down}} s_u + \eta_u, \tag{1}$$

where $\mathbf{h}_{l,u}^H$ is the channel from IRS to the u -th legitimate vehicle user, $\mathbf{h}_{l,u} \in \mathbb{C}^{G \times 1}$; Φ is the phase shift matrix, and $\Phi = \text{diag}\{e^{jX_g}\}$, $X_g \in [0, 2\pi)$, where X_g is the phase shift of the g -th ($\forall g \in \mathcal{G}$) reflection element; $\mathbf{H}_{B,l}$ is the channel from the RBS to IRS, $\mathbf{H}_{B,l} \in \mathbb{C}^{G \times N}$; s_u is the transmitted signal from the RBS for the u -th legitimate vehicle user with zero mean and normalized power; η_u is the noise received by the u -th legitimate vehicle user, $\eta_u \sim \mathcal{CN}(0, \sigma_u^2)$, where σ_u^2 is the noise power of the u -th legitimate vehicle user.

Similarly, the received signal y_u^{Eve} of the eavesdropper is

$$y_u^{\text{Eve}} = \mathbf{h}_{l,\text{Eve}}^H \Phi \mathbf{H}_{B,l} P_u^{\text{down}} s_u + \mathbf{h}_{l,\text{Eve}}^H \Phi \mathbf{h}_{l,u} P_u^{\text{up}} a_u + h_{u,\text{Eve}} P_u^{\text{up}} a_u + \eta_{\text{Eve}}, \tag{2}$$

where $\mathbf{h}_{l,\text{Eve}}^H$ is the channel from IRS to the eavesdropper, $\mathbf{h}_{l,\text{Eve}} \in \mathbb{C}^{G \times 1}$; a_u is the AN signal emitted by the u -th legitimate vehicle user with zero mean and normalized power; $h_{u,\text{Eve}}$ is the channel from the u -th legitimate vehicle user to the eavesdropper, $h_{u,\text{Eve}} \in \mathbb{C}$; η_{Eve} is the noise received by the eavesdropper, $\eta_{\text{Eve}} \sim \mathcal{CN}(0, \sigma_{\text{Eve}}^2)$, where σ_{Eve}^2 is the noise power of the eavesdropper.

According to (1), the information rate $R_{B,u}(\Phi, P_u^{\text{down}}, k_u)$ of the u -th legitimate vehicle user is given by

$$R_{B,u}(\Phi, P_u^{\text{down}}, k_u) = \sum_{k=1}^K B_u k_u \log_2(1 + \text{SINR}_{B,u}), \tag{3}$$

where B_u is the channel bandwidth of the u -th legitimate vehicle user, and $\text{SINR}_{B,u}$ can be expressed as

$$\text{SINR}_{B,u} = \frac{P_u^{\text{down}} |\mathbf{h}_{l,u}^H \Phi \mathbf{H}_{B,l}|^2}{\sigma_u^2}. \tag{4}$$

The information rate $R_{u,\text{Eve}}(\Phi, P_u^{\text{down}}, P_u^{\text{up}}, k_u)$ of the eavesdropper is given by

$$R_{u,\text{Eve}}(\Phi, P_u^{\text{down}}, P_u^{\text{up}}, k_u) = \sum_{k=1}^K B_{\text{Eve}} k_u \log_2(1 + \text{SINR}_{u,\text{Eve}}), \tag{5}$$

where $\text{SINR}_{u,\text{Eve}}$ can be expressed as

$$\text{SINR}_{u,\text{Eve}} = \frac{P_u^{\text{down}} |\mathbf{h}_{l,\text{Eve}}^H \Phi \mathbf{H}_{B,l}|^2}{P_u^{\text{up}} |\mathbf{h}_{l,\text{Eve}}^H \Phi \mathbf{h}_{u,l}|^2 + P_u^{\text{up}} |h_{u,\text{Eve}}|^2 + \sigma_{\text{Eve}}^2}. \tag{6}$$

For notational simplicity, we define Ψ_u as the power distribution coefficient of the u -th legitimate vehicle user. Since $P_u^{\text{max}} = P_u^{\text{down}} + P_u^{\text{up}}$, we have $P_u^{\text{down}} = \Psi_u P_u^{\text{max}}$ and $P_u^{\text{up}} = (1 - \Psi_u) P_u^{\text{max}}$. According to (3) and (5), in LAP-based IRS symbiotic VNETs, the secure channel capacity R_u^{sec} of the u -th legitimate vehicle user is

$$R_u^{\text{sec}}(\Phi, \Psi_u, k_u) = [R_{B,u}(\Phi, \Psi_u, k_u) - R_{u,\text{Eve}}(\Phi, \Psi_u, k_u)]^+, \tag{7}$$

where $[\cdot]^+$ represents $\max\{\cdot, 0\}$.

Therefore, the total secure channel capacity $R_{\text{tot}}^{\text{sec}}(\Phi, \Psi, \mathbf{K})$ can be expressed as

$$R_{\text{tot}}^{\text{sec}}(\Phi, \Psi, \mathbf{K}) = \sum_{u=1}^U R_u^{\text{sec}}(\Phi, \Psi_u, k_u), \tag{8}$$

where $\Psi = \{\Psi_u | \forall u \in \mathcal{U}\}$.

By optimizing the power distribution coefficient Ψ , phase shift Φ , and channel allocation policy \mathbf{K} , we aim to maximize the total secure channel capacity $R_{\text{tot}}^{\text{sec}}(\Phi, \Psi, \mathbf{K})$. The total secure channel capacity maximization problem can be mathematically formulated as

$$\mathbf{P1} : \max_{\Phi, \Psi, \mathbf{K}} R_{\text{tot}}^{\text{sec}}(\Phi, \Psi, \mathbf{K}) \tag{9a}$$

$$\text{s.t. } 0 < \Psi_u \leq 1, \forall u, \tag{9b}$$

$$\sum_{u=1}^U P_u^{\text{max}} = P_{\text{tot}}, \tag{9c}$$

$$\Phi = \text{diag}\{e^{jX_g}\}, \forall g, \tag{9d}$$

$$|e^{jX_g}| = 1, X_g \in [0, 2\pi), \forall g, \tag{9e}$$

$$k_u \in \{0, 1\}, \sum_{k=1}^K k_u = 1, \sum_{u=1}^U k_u \leq 1, \forall k, u, \tag{9f}$$

where P_{tot} is the total power of the system.

The main notations are summarized in Table 2.

Table 2. Definition of parameters.

Parameter	Definition
U	Number of legitimate vehicle users
G	Number of reflection elements
N	Number of antennas
K	Number of channels
P_u^{max}	Total power
P_u^{down}	Transmitted power of the RBS
P_u^{up}	Transmitted power of AN
y_u	Received signal of the u -th legitimate vehicle user
$\mathbf{h}_{l,u}^H$	Channel from IRS to the u -th legitimate vehicle user
Φ	Phase shift matrix
$\mathbf{H}_{B,l}$	Channel from the RBS to IRS
s_u	Transmitted signal from the RBS for the u -th legitimate vehicle user
$\mathbf{h}_{l,\text{Eve}}^H$	Channel from IRS to the eavesdropper
a_u	AN signal emitted by the u -th legitimate vehicle user
$h_{u,\text{Eve}}$	Channel from the u -th legitimate vehicle user to the eavesdropper
η_{Eve}	Noise received by the eavesdropper
$R_{B,u}$	Information rate of the u -th legitimate vehicle user
B_u	Channel bandwidth of the u -th legitimate vehicle user
$R_{u,\text{Eve}}$	Information rate of the eavesdropper
Ψ_u	Power distribution coefficient of the u -th legitimate vehicle user
R_u^{sec}	Secure channel capacity of the u -th legitimate vehicle user
$R_{\text{tot}}^{\text{sec}}$	Total secure channel capacity
P_{tot}	Total power of the system

In P1, (9b) and (9c) together limit the transmitted power of the RBS and legitimate vehicle users; (9d) and (9e) constrain the IRS phase shift; (9f) defines the channel allocation mode of multiple legitimate vehicle users. Since $|e^{jX_g}| = 1$ and $k_u \in \{0, 1\}$, P1 is a mixed-integer and non-convex program. It is hard to obtain a global optimal solution for P1. Therefore, in Section 3, we propose an iterative algorithm, where Ψ , Φ , and \mathbf{K} are solved in turn.

3. Total Secure Channel Capacity Maximization Scheme

3.1. Phase Shift Optimization

In this stage, given Ψ and \mathbf{K} , the phase shift optimization problem P2 is given by

$$\mathbf{P2} : \max_{\Phi} R_{\text{tot}}^{\text{sec}}(\Phi) = \sum_{u=1}^U R_u^{\text{sec}}(\Phi) \tag{10a}$$

$$\text{s.t. } \Phi = \text{diag}\{e^{jX_g}\}, \forall g, \tag{10b}$$

$$|e^{jX_g}| = 1, X_g \in [0, 2\pi), \forall g. \tag{10c}$$

Next, an intermediate variable \mathbf{X} is introduced, where $\mathbf{X} = [e^{jX_1}, \dots, e^{jX_G}]^H$. We have $\Phi = \text{diag}\{\mathbf{X}^H\}$. Let $\mathbf{A}_{l,u} = \text{diag}\{\mathbf{h}_{l,u}^H\}$ and $\mathbf{B}_{l,\text{Eve}} = \text{diag}\{\mathbf{h}_{l,\text{Eve}}^H\}$. Based on the property of matrix transformation (i.e., $\mathbf{a}^H \Phi \mathbf{b} = \mathbf{X}^H \text{diag}\{\mathbf{a}^H\} \mathbf{b}$), $\text{SINR}_u^{\text{sec}}(X)$ can be recast as

$$\text{SINR}_u^{\text{sec}}(X) = \frac{\mathbf{X}^H w_1 \mathbf{X}}{\mathbf{X}^H (w_2 + w_3 + w_4) \mathbf{X}} \times \mathbf{X}^H (w_5 + w_6) \mathbf{X}, \tag{11}$$

where $R_u^{\text{sec}}(\Phi) = \log_2[1 + \text{SINR}_u^{\text{sec}}(X)]$, and \mathbf{I}_G is the unit matrix. In addition, we have

$$w_1 = \left(\frac{1}{G}\right) \mathbf{I}_G + \frac{\Psi_u P_u^{\text{max}} (\mathbf{A}_{l,u} \mathbf{H}_{B,l} \mathbf{H}_{B,l}^H \mathbf{A}_{l,u}^H)}{\sigma_u^2}, \tag{12}$$

$$w_2 = \Psi_u P_u^{\text{max}} (\mathbf{B}_{l,\text{Eve}} \mathbf{H}_{B,l} \mathbf{H}_{B,l}^H \mathbf{B}_{l,\text{Eve}}^H), \tag{13}$$

$$w_3 = (1 - \Psi_u) P_u^{\text{max}} (\mathbf{B}_{l,\text{Eve}} \mathbf{h}_{l,u} \mathbf{h}_{l,u}^H \mathbf{B}_{l,\text{Eve}}^H), \tag{14}$$

$$w_4 = \left[\frac{(1 - \Psi_u) P_u^{\text{max}} |h_{u,\text{Eve}}|^2 + \sigma_{\text{Eve}}^2}{G} \right] \mathbf{I}_G, \tag{15}$$

$$w_5 = (1 - \Psi_u) P_u^{\text{max}} (\mathbf{B}_{l,\text{Eve}} \mathbf{h}_{l,u} \mathbf{h}_{l,u}^H \mathbf{B}_{l,\text{Eve}}^H), \tag{16}$$

and

$$w_6 = \left[\frac{(1 - \Psi_u) P_u^{\text{max}} |h_{u,\text{Eve}}|^2 + \sigma_{\text{Eve}}^2}{G} \right] \mathbf{I}_G. \tag{17}$$

To tackle P2, we further introduce three intermediate variables (α , β , and χ), which can be respectively expressed as

$$\alpha = \left(\frac{1}{G}\right) \mathbf{I}_G + \frac{\Psi_u P_u^{\text{max}} (\mathbf{A}_{l,u} \mathbf{H}_{B,l} \mathbf{H}_{B,l}^H \mathbf{A}_{l,u}^H)}{\sigma_u^2}, \tag{18}$$

$$\beta = \mathbf{B}_{l,\text{Eve}} \mathbf{H}_{B,l} \mathbf{H}_{B,l}^H \mathbf{B}_{l,\text{Eve}}^H, \tag{19}$$

and

$$\begin{aligned} \chi &= (1 - \Psi_u) P_u^{\text{max}} (\mathbf{B}_{l,\text{Eve}} \mathbf{h}_{l,u} \mathbf{h}_{l,u}^H \mathbf{B}_{l,\text{Eve}}^H) \\ &+ \left[(1 - \Psi_u) P_u^{\text{max}} |h_{u,\text{Eve}}|^2 + \sigma_{\text{Eve}}^2 \right] G^{-1} \mathbf{I}_G. \end{aligned} \tag{20}$$

Then, we simplify (11), and $\text{SINR}_u^{\text{sec}}(X)$ can be rewritten as

$$\text{SINR}_u^{\text{sec}}(X) = \frac{\text{tr}(\alpha \mathbf{X} \mathbf{X}^H) \text{tr}(\beta \mathbf{X} \mathbf{X}^H)}{\text{tr}(\chi \mathbf{X} \mathbf{X}^H)}, \tag{21}$$

where $\text{tr}(\cdot)$ is the trace of matrix.

To satisfy (10b) and (10c), we have

$$\begin{cases} \text{rank}(\mathbf{X} \mathbf{X}^H) = 1, \\ (\mathbf{X} \mathbf{X}^H)_{g,g} = 1, \forall g \in \mathcal{G}. \end{cases} \tag{22}$$

Afterward, a slack variable \mathfrak{S} is introduced. By using \mathfrak{S} , P2 can be rewritten as

$$\mathbf{P3} : \min_{\mathbf{X}} \mathfrak{S} \tag{23a}$$

$$\text{s.t. } e^{\log_2[\text{tr}(\chi \mathbf{X} \mathbf{X}^H)]} - \log_2[\text{tr}(\beta \mathbf{X} \mathbf{X}^H)] - \log_2[\text{tr}(\alpha \mathbf{X} \mathbf{X}^H)] - \mathfrak{S} \leq 0, \tag{23b}$$

$$\text{tr}(\alpha \mathbf{X} \mathbf{X}^H) \geq e^{\log_2[\text{tr}(\alpha \mathbf{X} \mathbf{X}^H)]}, \tag{23c}$$

$$\text{tr}(\beta \mathbf{X} \mathbf{X}^H) \geq e^{\log_2[\text{tr}(\beta \mathbf{X} \mathbf{X}^H)]}, \tag{23d}$$

$$\text{tr}(\chi \mathbf{X} \mathbf{X}^H) \leq e^{\log_2[\text{tr}(\chi \mathbf{X} \mathbf{X}^H)]}, \tag{23e}$$

$$\text{rank}(\mathbf{X} \mathbf{X}^H) = 1, \tag{23f}$$

$$(\mathbf{X} \mathbf{X}^H)_{g,g} = 1, \forall g. \tag{23g}$$

By using the sequential convex approximation (SCA) method, we take the first-order Taylor expansion of (23e), which can be expressed as

$$\begin{aligned} & e^{\log_2[\text{tr}(\chi \mathbf{X} \mathbf{X}^H)] - \Delta} + e^{\log_2[\text{tr}(\chi \mathbf{X} \mathbf{X}^H)] - \Delta} \ln[e(\Delta)] \\ & \leq e^{\log_2[\text{tr}(\chi \mathbf{X} \mathbf{X}^H)]} \Rightarrow \text{tr}(\chi \mathbf{X} \mathbf{X}^H) \\ & \leq e^{\log_2[\text{tr}(\chi \mathbf{X} \mathbf{X}^H)] - \Delta} (1 + \Delta), \end{aligned} \tag{24}$$

where Δ is a minuscule negative value. Therefore, $\{\log_2[\text{tr}(\chi \mathbf{X} \mathbf{X}^H)] - \Delta\}$ can be considered an approximation of $\log_2[\text{tr}(\chi \mathbf{X} \mathbf{X}^H)]$.

According to (24), we adopt the semi-definite relaxation (SDR) method to relax (23f). Under this condition, P3 can be relaxed as

$$\mathbf{P4} : \min_{\mathbf{X}} \mathfrak{S} \tag{25a}$$

$$\text{s.t. } (23b) - (23d), (23g) \tag{25b}$$

$$\text{tr}(\chi \mathbf{X} \mathbf{X}^H) \leq e^{\log_2[\text{tr}(\chi \mathbf{X} \mathbf{X}^H)] - \Delta} (1 + \Delta). \tag{25c}$$

Obviously, P4 is a convex optimization problem, which can be solved by the convex problem solver. However, since the SDR method is used to relax (23f), the obtained phase shift cannot always satisfy $\text{rank}(\mathbf{X} \mathbf{X}^H) = 1$ [27]. Therefore, the Gaussian random process is employed to acquire the approximate solution, which satisfies rank-one, i.e., $\text{rank}(\mathbf{X} \mathbf{X}^H) = 1$.

3.2. Power Distribution Coefficient Optimization

In this stage, since it is assumed that Φ and \mathbf{K} have been determined, the power distribution problem can be expressed as

$$P5 : \max_{\Psi} R_{\text{tot}}^{\text{sec}}(\Psi) = \sum_{u=1}^U R_u^{\text{sec}}(\Psi_u) \tag{26a}$$

$$\text{s.t. } 0 < \Psi_u \leq 1, \forall u, \tag{26b}$$

$$\sum_{u=1}^U P_u^{\text{max}} = P_{\text{tot}}. \tag{26c}$$

In P5, $\text{SINR}_u^{\text{sec}}(\Psi_u)$ can be rewritten as

$$\text{SINR}_u^{\text{sec}}(\Psi_u) = \frac{f_1 f_2}{P_u^{\text{max}}(f_3 - f_4) + \sigma_{\text{Eve}}^2}, \tag{27}$$

where $R_u^{\text{sec}}(\Psi_u) = \log_2[1 + \text{SINR}_u^{\text{sec}}(\Psi_u)]$. In addition, we can obtain

$$f_1 = \frac{1 + \Psi_u P_u^{\text{max}} \left(\mathbf{H}_{B,l}^H \Phi^H \mathbf{h}_{l,u} \mathbf{h}_{l,u}^H \Phi \mathbf{H}_{B,l} \right)}{\sigma_u^2}, \tag{28}$$

$$f_2 = (1 - \Psi_u) \left(P_u^{\text{max}} \left| \mathbf{h}_{l,\text{Eve}}^H \Phi \mathbf{h}_{l,u} \right|^2 + P_u^{\text{max}} |h_{u,\text{Eve}}|^2 \right) + \sigma_{\text{Eve}}^2, \tag{29}$$

$$f_3 = \left| \mathbf{h}_{l,\text{Eve}}^H \Phi \mathbf{h}_{l,u} \right|^2 + |h_{u,\text{Eve}}|^2, \tag{30}$$

and

$$f_4 = \Psi_u \left[\left| \mathbf{h}_{l,\text{Eve}}^H \Phi \mathbf{h}_{l,u} \right|^2 + |h_{u,\text{Eve}}|^2 - \left(\mathbf{H}_{B,l}^H \Phi^H \mathbf{h}_{l,\text{Eve}} \mathbf{h}_{l,\text{Eve}}^H \Phi \mathbf{H}_{B,l} \right) \right]. \tag{31}$$

Lemma 1. *The objective function $\text{SINR}_u^{\text{sec}}(\Psi_u)$ is a convex function.*

Proof of Lemma 1. The first-order derivative of $\text{SINR}_u^{\text{sec}}(\Psi_u)$ with respect to Ψ_u is derived as

$$\begin{aligned} \frac{\partial \text{SINR}_u^{\text{sec}}(\Psi_u)}{\partial \Psi_u} &= (\Psi_u)^2 \times (y_1 - y_2) \\ &- \frac{2 \left(\mathbf{H}_{B,l}^H \Phi^H \mathbf{h}_{l,u} \mathbf{h}_{l,u}^H \Phi \mathbf{H}_{B,l} \right) \left[P_u^{\text{max}} \left(\left| \mathbf{h}_{l,\text{Eve}}^H \Phi \mathbf{h}_{l,u} \right|^2 + |h_{u,\text{Eve}}|^2 \right) + \sigma_{\text{Eve}}^2 \right]}{\sigma_u^2 (P_u^{\text{max}})^{-2} \left[\left(\left| \mathbf{h}_{l,\text{Eve}}^H \Phi \mathbf{h}_{l,u} \right|^2 + |h_{u,\text{Eve}}|^2 \right) \right]^{-1} (\Psi_u)^{-1}} \\ &+ \frac{P_u^{\text{max}} \left(\mathbf{H}_{B,l}^H \Phi^H \mathbf{h}_{l,u} \mathbf{h}_{l,u}^H \Phi \mathbf{H}_{B,l} \right)}{\sigma_u^2 \left[P_u^{\text{max}} \left(\left| \mathbf{h}_{l,\text{Eve}}^H \Phi \mathbf{h}_{l,u} \right|^2 + |h_{u,\text{Eve}}|^2 \right) + \sigma_{\text{Eve}}^2 \right]^{-2}} \\ &- P_u^{\text{max}} \left(\mathbf{H}_{B,l}^H \Phi^H \mathbf{h}_{l,\text{Eve}} \mathbf{h}_{l,\text{Eve}}^H \Phi \mathbf{H}_{B,l} \right) \left[P_u^{\text{max}} \left(\left| \mathbf{h}_{l,\text{Eve}}^H \Phi \mathbf{h}_{l,u} \right|^2 + |h_{u,\text{Eve}}|^2 \right) + \sigma_{\text{Eve}}^2 \right], \end{aligned} \tag{32}$$

where

$$y_1 = \frac{(P_u^{\text{max}})^3 \left(\mathbf{H}_{B,l}^H \Phi^H \mathbf{h}_{l,u} \mathbf{h}_{l,u}^H \Phi \mathbf{H}_{B,l} \right)}{\sigma_u^2 \left(\left| \mathbf{h}_{l,\text{Eve}}^H \Phi \mathbf{h}_{l,u} \right|^2 + |h_{u,\text{Eve}}|^2 \right)^{-2}}, \tag{33}$$

and

$$y_2 = \frac{(P_u^{\max})^3 \left(\mathbf{H}_{B,l}^H \Phi^H \mathbf{h}_{l,u} \mathbf{h}_{l,u}^H \Phi \mathbf{H}_{B,l} \right) \left(\left| \mathbf{h}_{l,Eve}^H \Phi \mathbf{h}_{l,u} \right|^2 + |h_{u,Eve}|^2 \right)}{\sigma_u^2 \left(\mathbf{H}_{B,l}^H \Phi^H \mathbf{h}_{l,Eve} \mathbf{h}_{l,Eve}^H \Phi \mathbf{H}_{B,l} \right)^{-1}}. \tag{34}$$

The second-order derivative of $\text{SINR}_u^{\text{sec}}(\Psi_u)$ with respect to Ψ_u is derived as

$$\frac{\partial^2 \text{SINR}_u^{\text{sec}}(\Psi_u)}{\partial (\Psi_u)^2} = \frac{-2g_1 g_2}{(\Psi_u g_3 + g_4)^3}, \tag{35}$$

where

$$g_1 = P_u^{\max} \left(\mathbf{H}_{B,l}^H \Phi^H \mathbf{h}_{l,Eve} \mathbf{h}_{l,Eve}^H \Phi \mathbf{H}_{B,l} \right) \times \left[P_u^{\max} \left(\left| \mathbf{h}_{l,Eve}^H \Phi \mathbf{h}_{l,u} \right|^2 + |h_{u,Eve}|^2 \right) + \sigma_{Eve}^2 \right], \tag{36}$$

$$g_2 = P_u^{\max} \left(\left| \mathbf{h}_{l,Eve}^H \Phi \mathbf{h}_{l,u} \right|^2 + |h_{u,Eve}|^2 \right) - P_u^{\max} \left(\mathbf{H}_{B,l}^H \Phi^H \mathbf{h}_{l,Eve} \mathbf{h}_{l,Eve}^H \Phi \mathbf{H}_{B,l} \right) - \frac{P_u^{\max} \left(\mathbf{H}_{B,l}^H \Phi^H \mathbf{h}_{l,u} \mathbf{h}_{l,u}^H \Phi \mathbf{H}_{B,l} \right)}{\sigma_u^2 \left(P_u^{\max} \left(\left| \mathbf{h}_{l,Eve}^H \Phi \mathbf{h}_{l,u} \right|^2 + |h_{u,Eve}|^2 \right) + \sigma_{Eve}^2 \right)^{-1}}, \tag{37}$$

$$g_3 = P_u^{\max} \left(\mathbf{H}_{B,l}^H \Phi^H \mathbf{h}_{l,Eve} \mathbf{h}_{l,Eve}^H \Phi \mathbf{H}_{B,l} \right) - P_u^{\max} \left(\left| \mathbf{h}_{l,Eve}^H \Phi \mathbf{h}_{l,u} \right|^2 + |h_{u,Eve}|^2 \right), \tag{38}$$

and

$$g_4 = P_u^{\max} \left(\left| \mathbf{h}_{l,Eve}^H \Phi \mathbf{h}_{l,u} \right|^2 + |h_{u,Eve}|^2 \right) + \sigma_{Eve}^2. \tag{39}$$

We can obtain $g_1 > 0$, $g_2 > 0$, and $\Psi_u g_3 + g_4 > 0$. Therefore, we have $\frac{-2g_1 g_2}{(\Psi_u g_3 + g_4)^3} < 0$, i.e., $\frac{\partial^2 \text{SINR}_u^{\text{sec}}(\Psi_u)}{\partial (\Psi_u)^2} < 0$. In this case, the objective function $R_u^{\text{sec}}(\Psi_u)$ can be regarded as a convex function, thus proving Lemma 1. \square

According to Lemma 1, when $\frac{\partial^2 \text{SINR}_u^{\text{sec}}(\Psi_u)}{\partial (\Psi_u)^2} = 0$, we can obtain the maximum of $R_u^{\text{sec}}(\Psi_u)$. As can be seen from (32), $\frac{\partial^2 \text{SINR}_u^{\text{sec}}(\Psi_u)}{\partial (\Psi_u)^2}$ is a quadratic function with respect to Ψ_u . Therefore, $(\Psi_u)^*$ is derived as

$$(\Psi_u)^* = -\frac{g_4}{g_3} \pm \frac{\sqrt{g_1 g_2 g_5}}{g_3 g_5}, \tag{40}$$

where

$$g_5 = \frac{(P_u^{\max})^2 \left(\mathbf{H}_{B,l}^H \Phi^H \mathbf{h}_{l,u} \mathbf{h}_{l,u}^H \Phi \mathbf{H}_{B,l} \right)}{\sigma_u^2} \times \left(\left| \mathbf{h}_{l,Eve}^H \Phi \mathbf{h}_{l,u} \right|^2 + |h_{u,Eve}|^2 \right). \tag{41}$$

However, for $(\Psi_u)^* = -\frac{g_4}{g_3} + \frac{\sqrt{g_1 g_2 g_5}}{g_3 g_5}$, we have

$$\begin{aligned}
 (\Psi_u)^* &= -\frac{g_4}{g_3} + \frac{\sqrt{g_1 g_2 g_5}}{g_3 g_5} \geq -\frac{g_4}{g_3} \\
 &= \frac{P_u^{\max} \left(\left| \mathbf{h}_{l,Eve}^H \Phi \mathbf{h}_{l,u} \right|^2 + |h_{u,Eve}|^2 \right) + \sigma_{Eve}^2}{P_u^{\max} \left[\left(\left| \mathbf{h}_{l,Eve}^H \Phi \mathbf{h}_{l,u} \right|^2 + |h_{u,Eve}|^2 \right) - \left(\mathbf{H}_{B,l}^H \Phi^H \mathbf{h}_{l,Eve} \mathbf{h}_{l,Eve}^H \Phi \mathbf{H}_{B,l} \right) \right]} \\
 &\geq \frac{P_u^{\max} \left(\left| \mathbf{h}_{l,Eve}^H \Phi \mathbf{h}_{l,u} \right|^2 + |h_{u,Eve}|^2 \right) + \sigma_{Eve}^2}{P_u^{\max} \left(\left| \mathbf{h}_{l,Eve}^H \Phi \mathbf{h}_{l,u} \right|^2 + |h_{u,Eve}|^2 \right)} \\
 &= 1 + \frac{\sigma_{Eve}^2}{P_u^{\max} \left(\left| \mathbf{h}_{l,Eve}^H \Phi \mathbf{h}_{l,u} \right|^2 + |h_{u,Eve}|^2 \right)} > 1.
 \end{aligned} \tag{42}$$

According to (42), we know that $(\Psi_u)^* = -\frac{g_4}{g_3} + \frac{\sqrt{g_1 g_2 g_5}}{g_3 g_5}$ cannot satisfy (26b), i.e., $0 < \Psi_u \leq 1$. Under this condition, the optimal power distribution coefficient $(\Psi_u)^*$ is

$$(\Psi_u)^* \begin{cases} -\left(\frac{g_4}{g_3} + \frac{\sqrt{g_1 g_2 g_5}}{g_3 g_5} \right), & 0 < \Psi_u \leq 1, \\ 1, & \text{else.} \end{cases} \tag{43}$$

3.3. Channel Allocation

Similarly, we assume that Ψ and Φ have been given in advance. The channel allocation problem takes the form

$$\mathbf{P6} : \max_{\mathbf{K}} R_{\text{tot}}^{\text{sec}}(\mathbf{K}) = \sum_{u=1}^U R_u^{\text{sec}}(k_u) \tag{44a}$$

$$\text{s.t. } k_u \in \{0, 1\}, \sum_{k=1}^K k_u = 1, \sum_{u=1}^U k_u \leq 1, \forall k, u. \tag{44b}$$

As discussed in [23], P6 turns out to be a maximum weight bipartite matching (MWBM) problem. In polynomial time, the MWBM problem can be solved by the Hungarian algorithm. Based on above analysis, we can obtain the optimal channel allocation policy by using Algorithm 1.

Algorithm 1 Optimal channel allocation algorithm for P6

- 1: **for** $k = 1 : K$ **do**
 - 2: **for** $u = 1 : U$ **do**
 - 3: According to the SCA and SDR methods, as well as Gaussian random process, we can obtain the optimal phase shift $(\Phi)^*$.
 - 4: According to (43), we can acquire the optimal power distribution coefficient $(\Psi)^*$.
 - 5: We substitute $(\Phi)^*$ and $(\Psi)^*$ into (7) to obtain $R_u^{\text{sec}}(k_u)$.
 - 6: **end for**
 - 7: **end for**
 - 8: The Hungarian algorithm is adopted to solve P6.
 - 9: Output the optimal channel allocation policy $(\mathbf{K})^*$.
-

3.4. Overall Algorithmic Framework

In this paper, we design a total secure channel capacity maximization scheme for LAP and IRS enhanced transmissions, where the phase shift Φ , power distribution coefficient Ψ , and channel allocation \mathbf{K} are optimized. Figure 2 shows the overall algorithmic framework,

where Φ , Ψ , and \mathbf{K} are solved iteratively. Specifically, by using the SCA and SDR methods, we can solve the formulated phase shift optimization problem P2, based on which the optimal phase shift $(\Phi)^*$ satisfying the rank-one constraint can be obtained by adopting the Gaussian random process. Next, according to (43), we can obtain the closed-form expression of optimal power distribution coefficient $(\Psi)^*$. Then, Algorithm 1 employs the Hungarian algorithm to acquire $(\mathbf{K})^*$. Finally, the above processes are repeated until satisfying the termination condition.

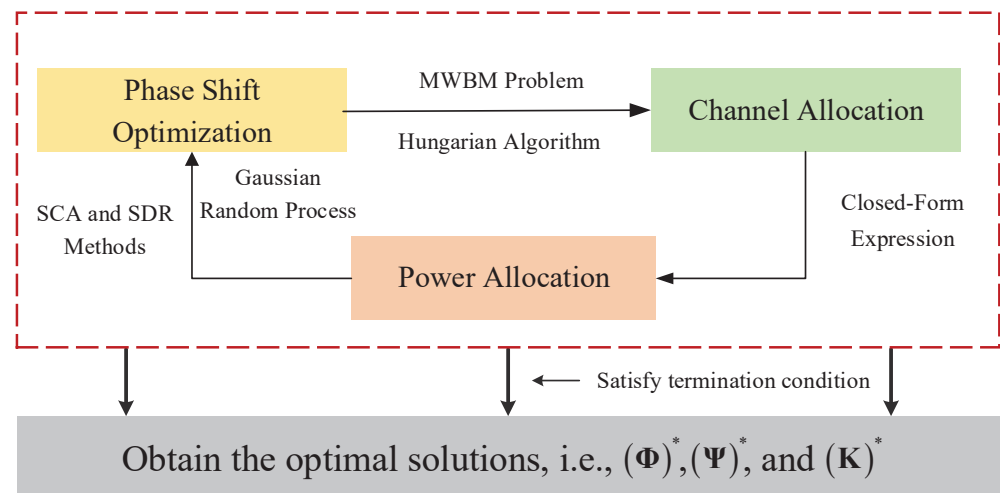


Figure 2. Overall algorithmic framework.

The complexity of the total secure channel capacity maximization scheme is mainly composed of three parts: (1) phase shift optimization; (2) power distribution coefficient optimization; (3) channel allocation. For the first part, since the SCA and SDR methods are used, the complexity of this part is $O(G^{3.5})$. Moreover, for the second part, we can derive the closed-form of the optimal power distribution coefficient; thus, the complexity of this part is $O(1)$. Furthermore, for the third part, the complexity of the channel allocation policy using the Hungarian algorithm is $O((U + K)^3)$. To summarize, the total computational complexity of solving P1 is $O(I_{\text{tot}}G^{3.5}) + O(I_{\text{tot}}) + O(I_{\text{tot}}(U + K)^3)$, where I_{tot} is the total number of iterations.

Discussion (Convergence Analysis): In this paper, the total secure channel capacity is maximized by iterative optimization. Therefore, the convergence needs to be analyzed. First, we present a simple scenario, which consists of an RBS, a fixed LAP equipped with IRS, a legitimate vehicle user, and an eavesdropper. In this case, $(\mathbf{K})^*$ can be obtained by using the enumeration method. As shown in Figure 3, for a given $(\mathbf{K})^*$, we iteratively optimize $(\Phi)^*$ and $(\Psi)^*$ based on the coordinated polling method. The objective function value (i.e., the total secure channel capacity) is improved partly after each iteration. Since the objective function value of P1 is bounded, our designed iterative algorithm can always converge to the optimal value or some certain values after finite iterations.

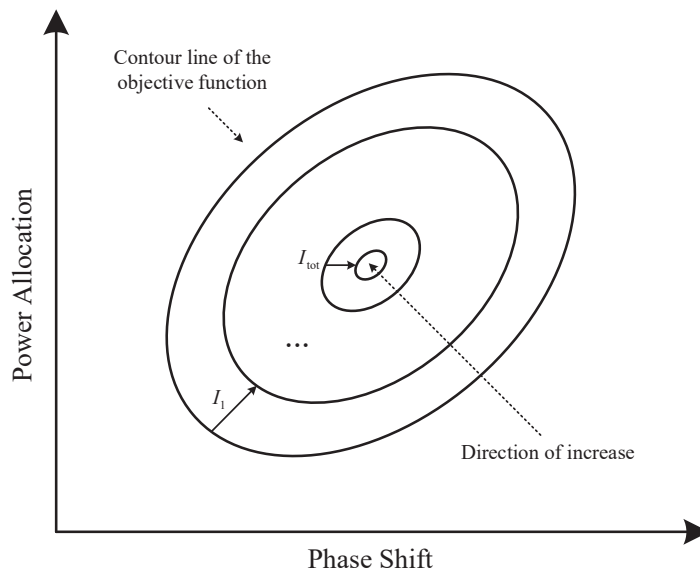


Figure 3. Coordinate polling method.

4. Performance Evaluation

In this section, simulation experiments are conducted to evaluate the performance of the proposed total secure channel capacity maximization scheme. Specifically, the comparison schemes are as follows. (a) Scheme 1 (LAP-PLS-CPO) [23]: This work uses the LAP to relay signals of the RBS and the PLS technique to ensure information security. In addition, the channel and power are optimized. (b) Scheme 2 (LAP-SPHO) [2]: This work adopts the LAP-enabled relay method to improve the data rate, based on which the spectrum, power, and LAP height are optimized. (c) Scheme 3 (LAP-RIS-CPO): In this scheme, Φ is initialized by random value, and then, \mathbf{K} and Ψ are optimized by the Algorithm 1 and (43), respectively.

In our simulations, we consider a scenario, where $U = [10, 55]$, $P_u^{\max} = 33$ dBm, $N = 32$, $K = [15, 60]$, $G = 64$, and $\sigma_u^2 = \sigma_{\text{Eve}}^2 = -174$ dBm/Hz. In order to analyze conveniently, a Cartesian coordinate is established in Figure 1, where the RBS is located at $(0, 0, 0)$ m, the fixed LAP equipped with IRS is located at $(800, 0, 200)$ m, the eavesdropper is located at $(650, 300, 0)$ m, and the cell radius of RBS is 1000 m. Moreover, the A2G channel model is $32.44 + 20 \lg[d(\text{km})] + 20 \lg[f_c(\text{MHz})]$. We model the fast fading channels as independent and identically distributed (i.i.d.) Rayleigh fading channels. As shown in Figure 1, the fast fading channels can be regarded as Rayleigh fading channels, taking into account the rich reflections and diffractions from surface-based obstacles.

Figure 4 illustrates the comparison of the total secure channel capacity with respect to the number of legitimate vehicle users under the different schemes. It is obvious that our proposed total secure channel capacity maximization scheme outperforms other comparison schemes. The reason is that the LAP and IRS enhanced transmissions are adopted in the considered scenario, based on which the phase shift, power distribution coefficient, and channel allocation are optimized. Compared to Scheme 1 (LAP-PLS-CPO), Scheme 2 (LAP-SPHO), and Scheme 3 (LAP-RIS-CPO), the total secure channel capacity can be increased by 67.56%, 141.3%, and 31.94%, respectively. Especially, for Scheme 2 (LAP-SPHO), since the PLS technique is not adopted, security cannot be satisfied, resulting in the lowest total secure channel capacity. In addition, even when the number of legitimate vehicle users is large, our designed scheme can still achieve relatively high information security rates.

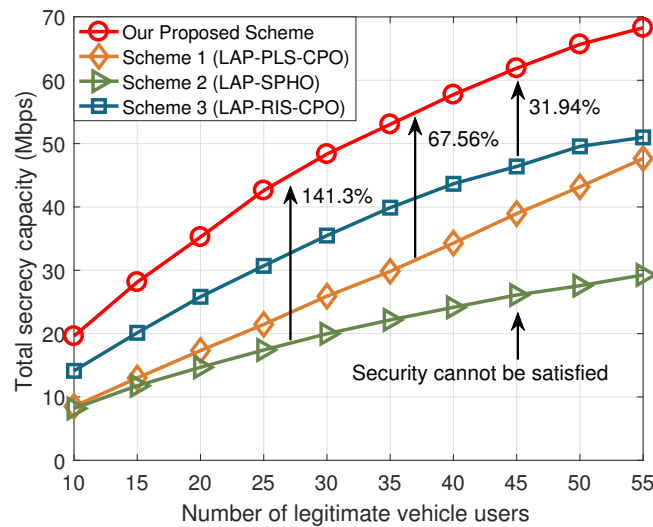


Figure 4. The total secure channel capacity versus the number of legitimate vehicle users.

Figure 5 shows the comparison of the total secure channel capacity with respect to the maximum transmitted power under the different schemes. We can observe that the total secure channel capacity increases monotonously with the increase in the maximum transmitted power P_u^{\max} . In addition, the larger the P_u^{\max} , the faster the growth of the total secure channel capacity. This is because, in this case, more power is allocated to AN to jam the eavesdropper, which can protect the security of 6G-oriented vehicular IoT services.

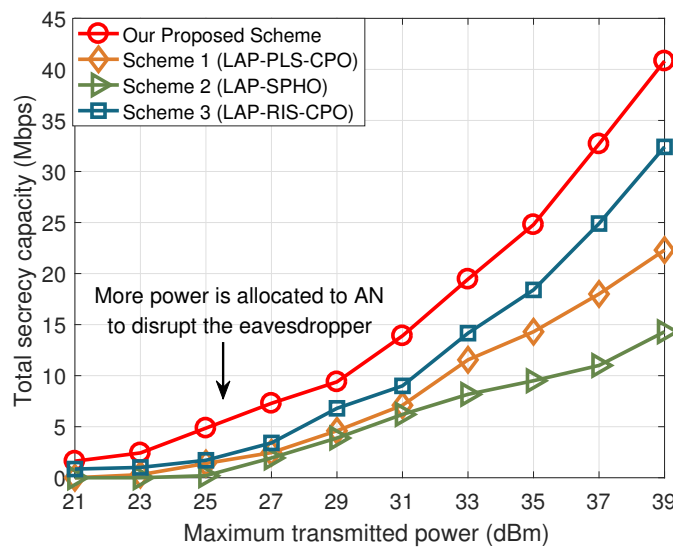


Figure 5. The total secure channel capacity versus the maximum transmitted power.

Next, we investigate the impact of the number of reflection elements on the performance of the proposed scheme. In Figure 6, we plot the comparison of the total secure channel capacity under different numbers of reflection elements. It is observed that the total secure channel capacity increases with the number of reflection elements. This phenomenon is more obvious when the number of legitimate vehicle users is small. This is because more reflection elements can better improve the channel quality. However, as discussed in Section 3.4, since the complexity of solving P2 is $O(G^{3.5})$, adding reflection elements will significantly increase the algorithm complexity. Therefore, there is a tradeoff between the total secure channel capacity and the algorithm complexity in terms of the number of reflection elements. The total secure channel capacity maximization by jointly considering the above two factors is a meaningful problem for future research.

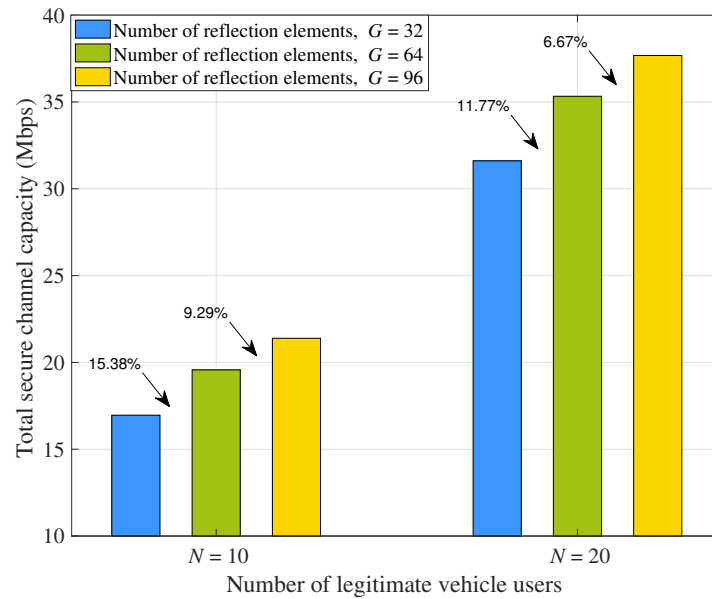


Figure 6. Comparison of the total secure channel capacity under different numbers of reflection elements.

As shown in Figure 7, we investigate the impact of the LAP's altitude on the total secure channel capacity. We can find that with the increase in the LAP's altitude, the total secure channel capacity decreases. The reason is that increasing the LAP's altitude will lead to an increase in the path loss, thereby reducing the total secure channel capacity. However, there is a minimum altitude limit for using this A2G channel model. For altitudes below 100 m, we need to change the large-scale fading model.

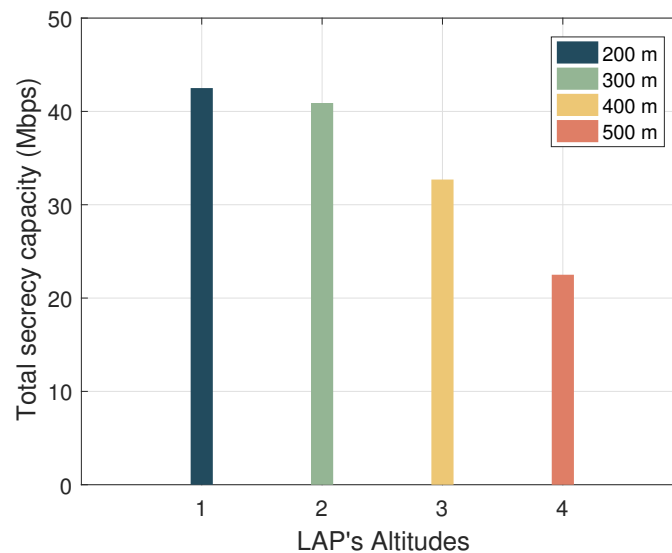


Figure 7. Comparison of the total secure channel capacity under different LAP altitudes.

As shown in Figure 8, we investigate the impact of the distance on the total secure channel capacity, where the LAP's X -axis positions are changed. It can be observed that the total secure channel capacity increases first and then decreases. Similarly, this is because the LAP's position will affect the path loss, thereby influencing the total secure channel capacity. Therefore, optimizing the LAP's deployment is an interesting topic that deserves further study.

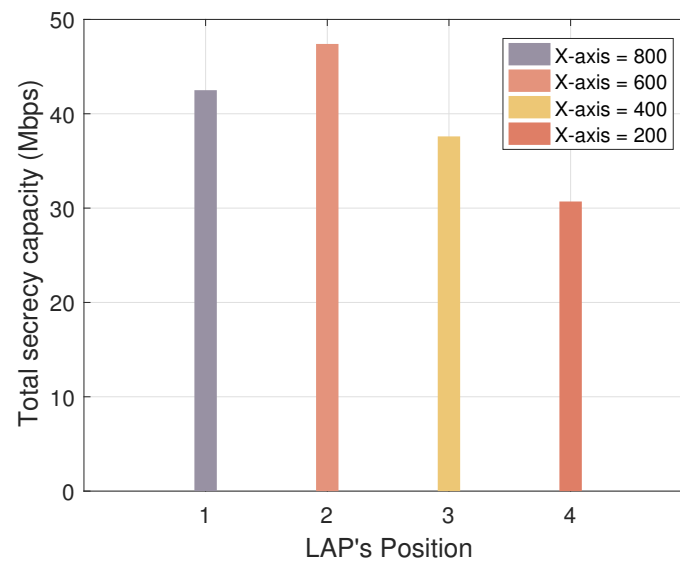


Figure 8. Comparison of the total secure channel capacity under different distances.

5. Conclusions

In order to improve the QoS of 6G-oriented vehicular IoT services, this paper used LAP equipped with IRS to overcome blockages, based on which the secure transmission problem was investigated. First, we introduced AN to enhance the security performance, which could prevent the eavesdropper from receiving privacy information. Next, by jointly considering the phase shift and power distribution coefficient optimization as well as channel allocation, we formulated a total secure channel capacity maximization problem for the LAP-based IRS symbiotic VNETs. Then, to deal with this intractable problem, we devised an iterative algorithm, based on which the convergence and the complexity were analyzed. Finally, numerical results demonstrated that the proposed scheme significantly outperformed the comparison schemes in terms of the total secure channel capacity. Furthermore, the joint optimization of the LAP location and network resources with imperfect CSI to maximize the total secure channel capacity is worth investigating and is challenging, which will be our future work.

Author Contributions: L.M.: Conceptualization, Methodology, Software, Writing—Original Draft Preparation, Visualization. J.L.: Conceptualization, Resources, Methodology, Software, Writing—Review. Y.H.: Conceptualization, Resources, Writing—Review and Editing, Supervision, Project Administration, Funding Acquisition. Q.S.: Conceptualization, Resources, Writing—Review. All authors have read and agreed to the published version of the manuscript.

Funding: This work was supported by the National Natural Science Foundation of China, under grant 62206221, and in part by the Fundamental Research Funds for the Central Universities.

Institutional Review Board Statement: Not applicable.

Informed Consent Statement: Not applicable.

Data Availability Statement: Not applicable.

Conflicts of Interest: The authors declare no conflict of interest for publishing in this journal.

References

1. Wang, C.; Li, Z.; Zhang, H.; Ng, D.W.K.; Al-Dhahir, N. Achieving covertness and security in broadcast channels with finite blocklength. *IEEE Trans. Wireless Commun.* **2022**, *21*, 7624–7640.
2. Zhai, D.; Li, H.; Tang, X.; Zhang, R.; Ding, Z.; Yu, F.R. Height optimization and resource allocation for NOMA enhanced UAV-aided relay networks. *IEEE Trans. Commun.* **2021**, *69*, 962–975.
3. Wang, C.; Li, Z.; Shi, J.; Ng, D.W.K. Intelligent reflecting surface-assisted multi-antenna covert communications: Joint active and passive beamforming optimization. *IEEE Trans. Commun.* **2021**, *69*, 3984–4000.

4. Fawaz, W. Effect of non-cooperative vehicles on path connectivity in vehicular networks: A theoretical analysis and UAV-based remedy. *Veh. Commun.* **2018**, *11*, 12–19. [[CrossRef](#)]
5. Fotouhi, A.; Qiang, H.; Ding, M.; Hasson, M.; Giordano, L.G.; Garcia-Rodriguez, A.; Yuan, J. Survey on UAV cellular communications: Practical aspects standardization advancements regulation and security challenges. *IEEE Commun. Surveys Tuts.* **2019**, *21*, 3417–3442.
6. Schweiger, K.; Preis, L. Urban air mobility: Systematic review of scientific publications and regulations for vertiport design and operation. *Drones* **2022**, *6*, 179.
7. Alsamhi, S.H.; Shvetsov, A.V.; Kumar, S.; Hassan, J.; Alhartomi, M.A.; Shvetsova, S.V.; Sahal, R.; Hawbani, A. Computing in the sky: A survey on intelligent ubiquitous computing for UAV-assisted 6G networks and industry 4.0/5.0. *Drones* **2022**, *6*, 177.
8. Cao, Y.; Lv, T.; Ni, W. Intelligent reflecting surface aided multi-user mmWave communications for coverage enhancement. In Proceedings of the 2020 IEEE 31st Annual International Symposium on Personal, Indoor and Mobile Radio Communications, London, UK, 31 August–3 September 2020; pp. 1–6
9. Pan, Q.; Wu, J.; Nebhen, J.; Bashir, A.K.; Su, Y.; Li, J. Artificial intelligence-based energy efficient communication system for intelligent reflecting surface-driven VANETs. *IEEE Trans. Intell. Transp. Syst.* **2022**, *23*, 19714–19726.
10. Zhi, K.; Pan, C.; Ren, H.; Wang, K. Power scaling law analysis and phase shift optimization of RIS-aided massive MIMO systems with statistical CSI. *IEEE Trans. Commun.* **2022**, *70*, 3558–3574.
11. You, C.; Kang, Z.; Zeng, Y.; Zhang, R. Enabling smart reflection in integrated air-ground wireless network: IRS meets UAV. *IEEE Wireless Commun.* **2021**, *28*, 138–144. [[CrossRef](#)]
12. Shafique, T.; Tabassum, H.; Hossain, E. Optimization of wireless relaying with flexible UAV-borne reflecting surfaces. *IEEE Trans. Commun.* **2021**, *69*, 309–325. [[CrossRef](#)]
13. Samir, M.; Elhattab, M.; Assi, C.; Sharafeddine, S.; Ghrayeb, A. Optimizing age of information through aerial reconfigurable intelligent surfaces: A deep reinforcement learning approach. *IEEE Trans. Veh. Technol.* **2021**, *70*, 3978–3983. [[CrossRef](#)]
14. Iacovelli, G.; Coluccia, A.; Grieco, L.A. Channel gain lower bound for IRS-assisted UAV-aided communications. *IEEE Commun. Lett.* **2021**, *25*, 3805–3809. [[CrossRef](#)]
15. Li, Y.; Zhang, H.; Long, K.; Nallanathan, A. Exploring sum rate maximization in UAV-based multi-IRS networks: IRS association, UAV altitude, and phase shift design. *IEEE Trans. Commun.* **2022**, *70*, 7764–7774. [[CrossRef](#)]
16. Al-Jarrah, M.; Al-Dweik, A.; Alsusa, E.; Iraqi, Y.; Alouini, M.-S. On the performance of IRS-assisted multi-layer UAV communications with imperfect phase compensation. *IEEE Trans. Commun.* **2021**, *69*, 8551–8568. [[CrossRef](#)]
17. Su, Y.; Pang, X.; Chen, S.; Jiang, X.; Zhao, N.; Yu, F.R. Spectrum and energy efficiency optimization in IRS-assisted UAV networks. *IEEE Trans. Commun.* **2022**, *70*, 6489–6502. [[CrossRef](#)]
18. Zhang, X.; Wang, J.; Poor, H.V. Joint optimization of IRS and UAV-trajectory: For supporting statistical delay and error-rate bounded QoS over mURLLC-driven 6G mobile wireless networks using FBC. *IEEE Veh. Technol. Mag.* **2022**, *17*, 55–63. [[CrossRef](#)]
19. Ji, Z.; Yang, W.; Guan, X.; Zhao, X.; Li, G.; Wu, Q. Trajectory and transmit power optimization for IRS-assisted UAV communication under malicious jamming. *IEEE Trans. Veh. Technol.* **2022**, *71*, 11262–11266. [[CrossRef](#)]
20. Wang, D.; He, T.; Zhou, F.; Cheng, J.; Zhang, R.; Wu, Q. Outage-driven link selection for secure buffer-aided networks. *Sci. China Inf. Sci.* **2022**, *65*, 182303. [[CrossRef](#)]
21. Sun, G.; Tao, X.; Li, N.; Xu, J. Intelligent reflecting surface and UAV assisted secrecy communication in millimeter-wave networks. *IEEE Trans. Veh. Technol.* **2022**, *70*, 11949–11961. [[CrossRef](#)]
22. Wang, D.; Wu, M.; He, Y.; Pang, L.; Xu, Q.; Zhang, R. An HAP and UAVs collaboration framework for uplink secure rate maximization in NOMA-enabled IoT networks. *Remote Sens.* **2022**, *14*, 4501. [[CrossRef](#)]
23. He, Y.; Nie, L.; Guo, T.; Kaur, K.; Hassan, M.M.; Yu, K. A NOMA-enabled framework for relay deployment and network optimization in double-layer airborne access VANETs. *IEEE Trans. Intell. Transp. Syst.* **2022**, *23*, 22452–22466. [[CrossRef](#)]
24. Ding, X.; Song, T.; Zou, Y.; Chen, X.; Hanzo, L. Security-reliability tradeoff analysis of artificial noise aided two-way opportunistic relay selection. *IEEE Trans. Veh. Technol.* **2017**, *66*, 3930–3941. [[CrossRef](#)]
25. Xu, S.; Liu, J.; Cao, Y. Intelligent reflecting surface empowered physical-layer security: Signal cancellation or jamming? *IEEE Internet Things J.* **2022**, *9*, 1265–1275. [[CrossRef](#)]
26. He, Y.; Wang, D.; Huang, F.; Zhang, R.; Gu, X.; Pan, J. A V2I and V2V collaboration framework to support emergency communications in ABS-aided Internet of Vehicles. *IEEE Trans. Green Commun. Netw.* **2023**, *Early access*. [[CrossRef](#)]
27. Luo, Z.; Ma, W.; So, A.M.; Ye, Y.; Zhang, S. Semidefinite relaxation of quadratic optimization problems. *IEEE Signal Process. Mag.* **2010**, *27*, 20–34. [[CrossRef](#)]

Disclaimer/Publisher’s Note: The statements, opinions and data contained in all publications are solely those of the individual author(s) and contributor(s) and not of MDPI and/or the editor(s). MDPI and/or the editor(s) disclaim responsibility for any injury to people or property resulting from any ideas, methods, instructions or products referred to in the content.